Photophysics of the Fluorescent K^+ Indicator PBFI

Katrien Meuwis,* Noël Boens,* Frans C. De Schryver,* Jacques Gallay,‡ and Michel Vincent‡
*Department of Chemistry, Katholieke Universiteit Leuven, Heverlee, Belgium; and ‡Laboratoire pour l'Utilisation du Rayonnement Electromagnétique, Centre Universitaire Paris-Sud, Orsay, France

ABSTRACT The fluorescent indicator PBFI is widely used for the determination of intracellular concentrations of K^+. To investigate the binding reaction of K^+ to PBFI in the ground and excited states, steady-state and time-resolved measurements were performed. The fluorescence decay surface was analyzed with global compartmental analysis yielding the following values for the rate constants at room temperature in aqueous solution at pH 7.2: $k_{01} = 1.1 \times 10^9\ s^{-1}$, $k_{21} = 2.7 \times 10^8\ M^{-1}s^{-1}$, $k_{02} = 1.8 \times 10^9\ s^{-1}$, and $k_{12} = 1.4 \times 10^9\ s^{-1}$. k_{01} and k_{02} denote the respective deactivation rate constants of the K^+ free and bound forms of PBFI in the excited state. k_{21} represents the second-order rate constant of binding of K^+ to the indicator in the excited state whereas k_{12} is the first-order rate constant of dissociation of the excited K^+-PBFI complex. From the estimated values of k_{12} and k_{21}, the dissociation constant K_d^* in the excited state was calculated. It was found that pK_d^* (–0.7) is smaller than pK_d (2.2). The effect of the excited-state reaction can be neglected in the determination of K_d and/or the K^+ concentration. Therefore, intracellular K^+ concentrations can be accurately determined from fluorimetric measurements by using PBFI as K^+ indicator.

INTRODUCTION

PBFI is a selective ion indicator for the fluorimetric determination of intracellular K^+ concentrations. PBFI consists of two benzofuran isophthalate fluorophores linked to the nitrogens of a diazacrown ether with a cavity size that confers selectivity for K^+ (Fig. 1). In the absence of K^+ at pH 7, the extinction coefficient is approximately 42,000 $M^{-1}\ cm^{-1}$ at 345 nm. K^+ binds to PBFI with a 1:1 stoichiometry and a ground-state dissociation constant K_d of 8 mM in the absence of Na^+. There is a strong dependence of Na^+ on the K^+ affinity of PBFI; K_d is approximately 100 mM in the presence of Na^+ (Minta and Tsien, 1989). The fluorescence is relatively unaffected by changes in pH between 6.5 and 7.5. Although PBFI is only 1.5-fold more selective for K^+ than for Na^+, PBFI can be used for intracellular [K^+] determinations because there is normally 10 times more K^+ than Na^+ in cells. Binding of K^+ induces a 2.5-fold enhancement of fluorescence intensity. Furthermore, the excitation and emission maxima of PBFI shift to shorter wavelengths. The ratio of the fluorescence signals obtained by exciting PBFI at 340–345 nm and at 370–390 nm while monitoring the fluorescence at 450–550 nm is used to determine the intracellular K^+ concentration.

It is not generally acknowledged that the binding reaction of K^+ to PBFI and the corresponding dissociation of the formed complex also occur in the excited state. This may lead to an erroneous value of K_d derived from fluorimetric measurements. As a consequence, the intracellular K^+ concentration may also be incorrect. The degree of interference of the excited-state reaction on the determination of K_d and/or [K^+] depends on the values of the four rate constants defining the excited-state reaction (Kowalczyk et al., 1994). These values can be assessed by the one-step global compartmental analysis (Ameloot et al., 1991, 1992) of the fluorescence decay surface of PBFI as a function of [K^+].

Before any new fluorescent molecule is proposed as a fluorescent indicator for biologically important species, time-resolved fluorescence measurements should be performed to estimate values of the four rate constants defining the excited-state reaction. Using these values allows one to predict whether the determination of K_d from fluorimetric titration is undisturbed by the excited-state reaction. This general approach is exemplified here for the binding reaction of PBFI and K^+. Application of the analytical expressions for the fluorescence signal in the absence and presence of an excited-state reaction indicate that the determination of K_d and/or [K^+] is not influenced by the excited-state complex formation and dissociation.

THEORY

Kinetics

Consider a causal, linear, time-invariant, intermolecular system consisting of two distinct types of ground-state species and two corresponding excited-state species as is depicted in Scheme 1a. Ground-state species 1 can reversibly react with M to form ground-state species 2. In the case of PBFI, species I represents the ground state of the free form of the indicator, species 2 is the ground state of the complex between K^+ and PBFI, and M denotes the K^+ ion (see Scheme 1b). Excitation by light creates the excited-state species 1* and 2*, which can decay by fluorescence (F) and nonradiative (NR) processes (internal conversion (IC) and intersystem crossing (ISC)). The composite rate constant for these processes are denoted by k_{0i} ($=k_{Fi} + k_{NRi} = k_{Fi} + k_{ICi} + k_{ISCi}$) for species i*. The second-order rate constant describing the transformation

Received for publication 5 July 1994 and in final form 10 March 1995.
Address reprint requests to Dr. Noel Boens, Department of Chemistry, Katholieke Universiteit Leuven, B-3001 Heverlee, Belgium. Tel.: 011-32-16-327497; Fax: 011-32-16-327990, E-mail: Noel.Boens@chem.kuleuven.ac.be.

0006-3495/95/06/2469/05 $2.00

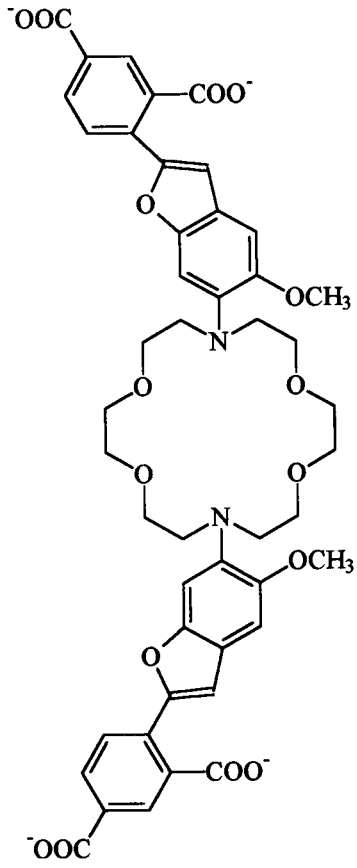

FIGURE 1 Chemical structure of the potassium indicator PBFI.

$1^* + M \rightarrow 2^*$ is represented by k_{21}. The first-order rate constant for the dissociation of 2^* into 1^* and M is denoted by k_{12}.

If the system depicted in Scheme 1 is excited by a δ-pulse that does not significantly alter the concentrations of the ground-state species, the fluorescence δ-response function, $f(\lambda^{em}, \lambda^{ex}, t)$, measured at emission wavelength λ^{em} due to excitation at λ^{ex} is expressed by (Ameloot et al., 1991)

$$f(\lambda^{em}, \lambda^{ex}, t) = \kappa\, \tilde{\mathbf{c}}(\lambda^{em})\mathbf{U} \exp(t\Gamma)\mathbf{U}^{-1}\tilde{\mathbf{b}}(\lambda^{ex}), \qquad t \geq 0, \tag{1}$$

with κ a proportionality constant. $\mathbf{U} = [\mathbf{U}_1, \mathbf{U}_2]$ is the matrix of the two eigenvectors of matrix $\mathbf{A}$ (Eq. 2) and $\mathbf{U}^{-1}$ the inverse of $\mathbf{U}$. γ_1 and γ_2 are the eigenvalues of $\mathbf{A}$ corresponding to $\mathbf{U}_1$ and $\mathbf{U}_2$, and $\exp(t\Gamma) = \mathrm{diag}\{\exp(\gamma_1 t), \exp(\gamma_2 t)\}$.

$$\mathbf{A} \equiv \begin{bmatrix} -(k_{01} + k_{21}[\mathrm{M}]) & k_{12} \\ k_{21}[\mathrm{M}] & -(k_{02} + k_{12}) \end{bmatrix}. \tag{2}$$

$\mathbf{b}$ is the 2×1 vector of the normalized absorbances $\tilde{b}_i$ of species i at λ^{ex} (Ameloot et al., 1991):

$$\tilde{b}_i = b_i/(b_1 + b_2) \qquad \text{for} \quad i = 1, 2. \tag{3}$$

$\tilde{\mathbf{b}}$ is dependent on λ^{ex} and [M].

$\tilde{\mathbf{c}}$ is the 1×2 vector of the normalized spectral emission weighting factors $\tilde{\mathbf{c}}_i$ of species $\mathbf{i}^*$ at λ^{em} (Ameloot et al., 1991):

$$\tilde{c}_i = c_i/(c_1 + c_2) \qquad \text{for} \quad i = 1, 2. \tag{4}$$

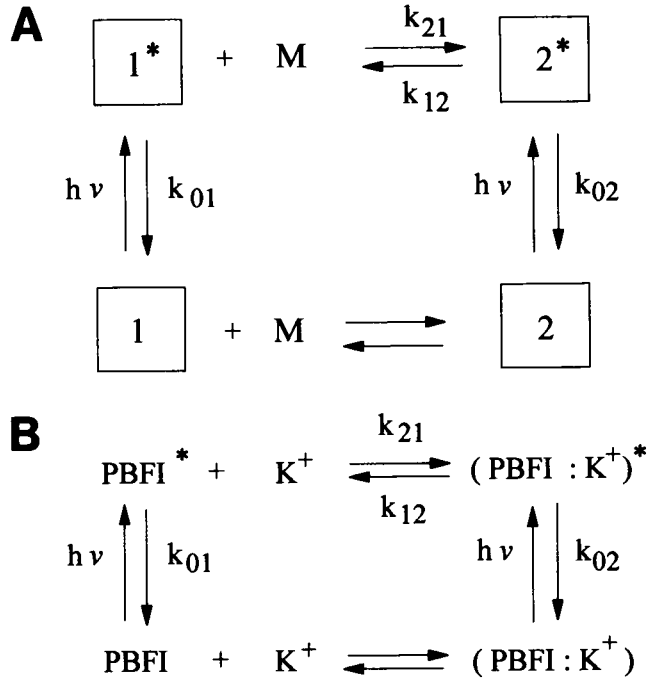

Scheme 1

$\tilde{\mathbf{b}}$ $(\lambda^{ex}, [\mathrm{M}])$ can be linked over decay curves collected at the same excitation wavelength and [M], whereas $\tilde{\mathbf{c}}(\lambda^{em})$ can be linked over decay curves obtained at the same emission wavelength.

Equation 1 can be written in the biexponential format:

$$f(\lambda^{em}, \lambda^{ex}, t) = \alpha_1(\lambda^{em}, \lambda^{ex})\exp(\gamma_1 t) + \alpha_2(\lambda^{em}, \lambda^{ex})\exp(\gamma_2 t), \qquad t \geq 0. \tag{5}$$

The exponential factors $\gamma_{1,2}$ are related to the decay times $\tau_{1,2}$ according to

$$\gamma_{1,2} = -1/\tau_{1,2} \tag{6}$$

and are given by

$$\gamma_{1,2} = -\tfrac{1}{2}\{S_1 + S_2 \mp [(S_1 - S_2)^2 + 4\, k_{21}k_{12}[\mathrm{M}]]^{1/2}\}, \tag{7}$$

with

$$S_1 = k_{01} + k_{21}[\mathrm{M}] \tag{8a}$$

$$S_2 = k_{02} + k_{12}. \tag{8b}$$

For clarity, we shall not use the notation τ_1 and τ_2, but we shall refer to τ_L (L for long) and τ_S (S for short) with $\tau_L > \tau_S$.

Fluorimetric titration

For the compartmental system depicted in Scheme 1, the measured steady-state fluorescence signal $F(\lambda^{em}, \lambda^{ex}, [\mathrm{M}])$ due to excitation at λ^{ex} and observed at λ^{em} is given by (Ameloot et al., 1991; Kowalczyk et al., 1994)

$$F(\lambda^{em}, \lambda^{ex}, [\mathrm{M}]) = -\xi(\lambda^{em})\mathbf{c}(\lambda^{em})\, \mathbf{A}^{-1}\, \mathbf{b}(\lambda^{ex}, [\mathrm{M}]) \tag{9}$$

where $\xi(\lambda^{em})$ is an instrumental factor. If Beer's law is obeyed and if the absorbance of the solution is low (<0.1), then the elements $\mathbf{b}_i$ (λ^{ex}, [M]) of $\mathbf{b}$ can be approximated as

$$b_i(\lambda^{ex}, [M]) \approx 2.3d\,\epsilon_i(\lambda^{ex})\,[i]I_0(\lambda^{ex}) \tag{10}$$

where d denotes the excitation light path, $I_0(\lambda^{ex})$ represents the concentration (in mol/L) of excitation photons of wavelength λ^{ex} impinging on the sample, and $\epsilon_i(\lambda^{ex})$ is the molar extinction coefficient for species i at excitation wavelength λ^{ex}. In that case, Eq. 9 is explicitly given by (Kowalczyk et al., 1994)

$$F(\lambda^{em}, \lambda^{ex}, [M]) = 2.3d\,I_0(\lambda^{ex})\xi(\lambda^{em})\frac{a_1\epsilon_1 K_d + a_2\epsilon_2[M]}{K_d + [M]}C_T. \tag{11}$$

$a_1(\lambda^{em})$ and $a_2(\lambda^{em})$ are defined by

$$a_1(\lambda^{em}) = \frac{(k_{02} + k_{12})c_1(\lambda^{em}) + k_{21}[M]c_2(\lambda^{em})}{k_{01}(k_{02} + k_{12}) + k_{02}k_{21}[M]} \tag{12a}$$

$$a_2(\lambda^{em}) = \frac{k_{12}c_1(\lambda^{em}) + (k_{01} + k_{21}[M])c_2(\lambda^{em})}{k_{01}(k_{02} + k_{12}) + k_{02}k_{21}[M]}. \tag{12b}$$

K_d is the ground-state dissociation constant expressed in the form of molar concentrations:

$$K_d = [1][M]/[2]. \tag{13}$$

$C_T = [1] + [2]$ represents the total analytical concentration of the fluorescent probe. It must be emphasized that the functional dependence of F (Eq. 11) on $-\log[M]$ is very complicated and cannot be used to determine K_d (Kowalczyk et al., 1994). The knowledge of the four rate constants (k_{01}, k_{21}, k_{02}, and k_{12}) determining the excited-state reaction allows one to calculate $a_{1,2}$ according to Eq. 12 and hence to determine the concentration range of M where interference of the excited-state reaction is significant.

Without an excited-state reaction (i.e., $k_{21} = 0$ and $k_{12} = 0$), the expressions for $a_{1,2}$ simplify:

$$a_1(\lambda^{em}) = \frac{c_1(\lambda^{em})}{k_{01}} \tag{14a}$$

$$a_2(\lambda^{em}) = \frac{c_2(\lambda^{em})}{k_{02}}. \tag{14b}$$

The plot of F versus $-\log[M]$ exhibits a unique inflection point at $[M] = K_d$. Equation 11 can now be rewritten in the form of a Hill plot,

$$\log\left(\frac{F - F_{min}}{F_{max} - F}\right) = \log[M] - \log K_d \tag{15}$$

from which K_d can be determined.

MATERIALS AND METHODS

Materials

PBFI, tetraammonium salt was obtained from Molecular Probes (Eugene, OR). MOPS (3-(*N*-morpholino)propanesulfonic acid) free acid was purchased from Sigma Chemie (Bornem, Belgium), and KCl from Aldrich Chimica (Geel, Belgium). All products were used as received. Fluorimetric measurements were performed with aqueous buffer solutions of 4.208 μM PBFI in the presence of KCl (up to 4.03 M). All measurements were done at room temperature. Solutions of KOH and MOPS were used to obtain the physiological pH value of 7.2. Milli-Q water was used to prepare the aqueous solutions according to the procedure described by Minta and Tsien (1989). The ionic strength of solutions with different $[K^+]$ was not kept constant.

Instrumentation

Fully corrected steady-state excitation and emission spectra were recorded on a SPEX Fluorolog 212.

The fluorescence decay traces were collected by the single photon timing technique (O'Connor and Phillips, 1984; Boens, 1991) by using the synchrotron radiation facility SUPER-ACO (Anneau de Collision d'Orsay at LURE, France) as described elsewhere (Kuipers et al., 1991). The storage ring provides vertically polarized light pulses with a full width at half maximum of ≈500 ps at a frequency of 8.33 MHz in double bunch mode. A Hamamatsu microchannel plate R1564U-06 was utilized to detect the fluorescence photons under magic angle (54° 44′). The instrument response function was determined by measuring the light scattered by glycogen in aqueous solution at the emission wavelength. All decay traces were collected in 1/2K channels of a multichannel analyzer and contained approximately 5×10^3 peak counts. The time increment per channel was 5.8 ps.

Data analysis

The global compartmental analysis of the fluorescence decay surface of species undergoing excited-state processes was implemented in the existing general global analysis program (Boens et al., 1989) based on the algorithm of Marquardt (1963). The global fitting parameters are k_{01}, k_{21}, k_{02}, k_{12}, $\tilde{b}_1$, and $\tilde{c}_1$. The rate constants k_{01}, k_{21}, k_{02}, and k_{12} are the same for all decays. In contrast, the coefficients $\tilde{c}_1$ are expected to be identical for those decays observed at the same emission wavelength. The normalized ground-state absorbances $\tilde{b}_1$ are identical for the decays at the same excitation wavelength and K^+ concentration. For each decay curve additionally a local scaling factor has to be estimated. Specifying $[K^+]$ and assigning initial guesses to the rate constants k_{01}, k_{21}, k_{02}, and k_{12} allows one to construct the matrix **A** (Eq. 2) for each decay trace. The eigenvalues γ and the associated eigenvectors **U** of this matrix are determined with routines from EISPACK, Matrix Eigensystem Routines (Smith et al., 1974). The eigenvectors are then scaled to the initial conditions $\tilde{\mathbf{b}}$. The preexponential factors α are computed from the rate constants, $[K^+]$, $\tilde{b}$, and $\tilde{c}$, allowing the calculation of the fluorescence decay of the sample. By using this approach, all decay traces collected at different excitation/emission wavelengths and at different K^+ concentrations are linked by all rate constants defining the system and can therefore be analyzed simultaneously by the model given by Eq. 1.

The fitting parameters were determined by minimizing the global reduced χ_g^2:

$$\chi_g^2 = \sum_{l}^{q}\sum_{i} w_{li}\,(y_{li}^o - y_{li}^c)^2/\nu \tag{16}$$

where the index l sums over q experiments, and the index i sums over the appropriate channel limits for each individual experiment. y_{li}^o and y_{li}^c denote, respectively, the experimentally measured and fitted values corresponding to the ith channel of the lth experiment. w_{li} is the corresponding statistical weight. ν represents the number of degrees of freedom for the entire multidimensional fluorescence decay surface. The statistical criteria to judge the quality of the fit comprised both graphical and numerical tests. The graphical methods included plots of surfaces (carpets) of the autocorrelation function values versus experiment number and of the weighted residuals versus channel number versus experiment number. χ_g^2 and its corresponding $Z_{\chi_g^2}$ (Eq. 17) provide numerical goodness-of-fit criteria for the entire fluorescence decay surface.

$$Z_{\chi_g^2} = (\chi_g^2 - 1)(1/2\,\nu)^{1/2} \tag{17}$$

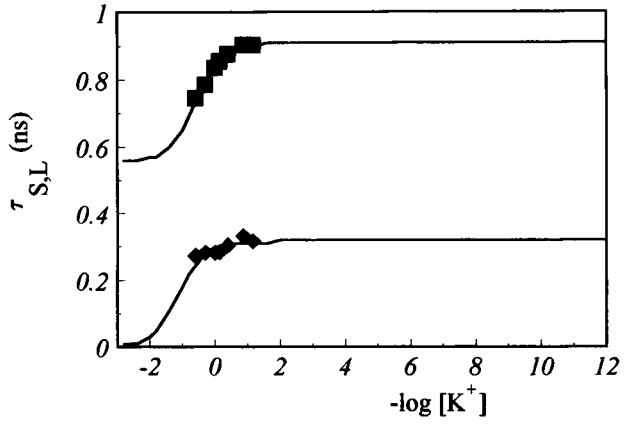

FIGURE 2 Decay times (—) of PBFI as a function of $-\log[K^+]$ calculated according to Eqs. 6–8 with the rate constant values obtained from global compartmental analysis (Table 2). The symbols ■ and ♦ represent the decay times estimated by global biexponential analysis.

By using $Z_{\chi_g^2}$ the goodness-of-fit of analyses with different ν can be readily compared. The additional criteria to judge the quality of the fits are described elsewhere (Boens, 1991). Standard error estimates were obtained from the parameter covariance matrix available from the analysis. All quoted errors are one standard deviation. All analyses were performed on an IBM RISC System/6000 computer.

RESULTS

The ground-state dissociation constant K_d of the K^+-PBFI complex was determined from a Hill plot by using fluorescence measurements at λ^{ex} = 350 nm, at 20°C, pH 7.2, in aqueous solution. The Hill plot yielded a value of 6.62 mM for K_d (corresponding to $pK_d = 2.18 \pm 0.04$) and indicated a 1:1 stoichiometry (slope = 0.96 ± 0.04) for the K^+-PBFI complex. To determine values of the rate constants k_{01}, k_{21}, k_{02}, and k_{12}, time-resolved fluorescence measurements were performed. The decay traces of PBFI at seven different concentrations of K^+ ranging from 68.8 mM to 4.03 M were measured at two different excitation wavelengths (λ^{ex} = 340 nm, 350 nm) and two different emission wavelengths (λ^{em} = 510 nm, 530 nm).

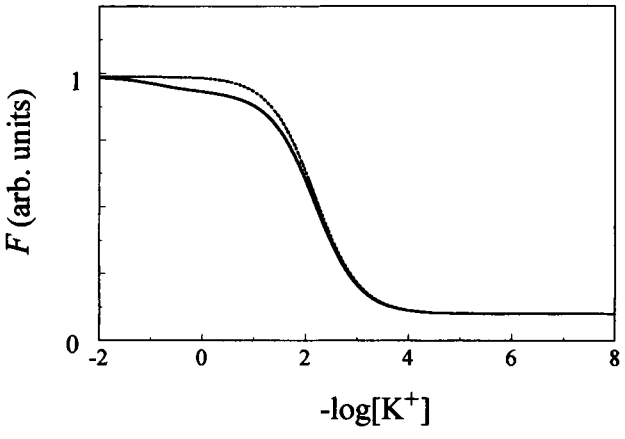

FIGURE 3 Fluorimetric titration curves F computed in the absence (—) and presence (- - -) of an excited-state reaction at λ^{em} = 510 nm with λ^{ex} = 345 nm and λ^{ex} = 385 nm. The rate constants of Table 2 were used together with the following experimentally determined values of K_d = 6.62 mM; ϵ_1 = 28,000 M^{-1} cm^{-1}; ϵ_2 = 37,000 M^{-1} cm^{-1} at λ^{ex} = 345 nm; ϵ_1 = 3,500 M^{-1} cm^{-1} and ϵ_2 = 3,900 M^{-1} cm^{-1} at λ^{ex} = 385 nm; $c_1/(c_1 + c_2)$ = 0.37 and $c_2/(c_1 + c_2)$ = 0.63.

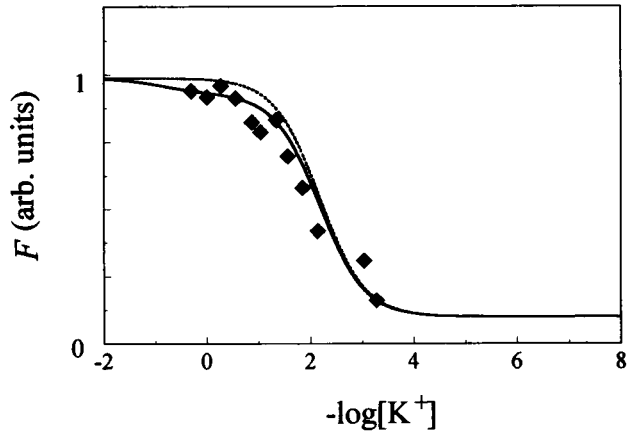

FIGURE 4 Experimental (♦) fluorimetric titration curve F(510 nm, 345 nm) for PBFI at pH 7.2 in aqueous solution at room temperature. The solid line represents the F(510 nm, 345 nm) values calculated with K_d = 6.62 mM, ϵ_1 = 28,000 M^{-1} cm^{-1}, and ϵ_2 = 37,300 M^{-1} cm^{-1} at λ^{ex} = 345 nm; $c_1/(c_1 + c_2)$ = 0.37, $c_2/(c_1 + c_2)$ = 0.63 at 510 nm assuming the presence (—) or absence (- - -) of an excited-state reaction. The used rate constant values are those of Table 2.

The decays arising from solutions with identical K^+ concentrations were analyzed globally as biexponential functions (Eqs. 5–10) in terms of preexponential factors and decay times. The decay times are linked over the emission and excitation wavelengths at each concentration of K^+. Global biexponential analysis gave good fits over the whole concentration range even at K^+ concentrations of 135 mM or higher, when the indicator is saturated in the ground state. The results of the global biexponential analyses are compiled in Table 1.

From this table it is clear that for increasing $[K^+]$ both decay times decrease, indicating that $k_{01} < k_{02}$ (Van den Bergh et al., 1994). It has been shown before (Van den Bergh et al., 1994) that τ_L equals $1/k_{01}$ whereas τ_S equals $1/(k_{02} + k_{12})$ at low $[K^+]$.

In global compartmental analysis all the decay traces were analyzed simultaneously, resulting in the rate constant values that are shown in Table 2. The values of the rate constants estimated by global compartmental analysis confirm the results of global biexponential analysis, namely: $1/k_{01}$ = 0.907 ns $\approx \tau_L$ and $1/(k_{02} + k_{12})$ = 0.312 $\approx \tau_S$ at low $[K^+]$.

TABLE 1 Globally estimated decay times of PBFI at different K^+ concentrations

$[K^+]$	τ_S (ns)	τ_L (ns)	n*	$Z_{\chi_g^2}$	χ_g^2
68.8 mM	0.316 ± 0.002	0.903 ± 0.001	6	2.60	1.04
136.9 mM	0.332 ± 0.002	0.804 ± 0.001	6	−0.86	0.99
406.8 mM	0.304 ± 0.002	0.876 ± 0.001	6	−1.18	0.98
737.2 mM	0.284 ± 0.002	0.855 ± 0.001	6	−0.63	0.99
1.02 M	0.282 ± 0.002	0.836 ± 0.001	6	−0.01	1.00
2.02 M	0.282 ± 0.002	0.785 ± 0.001	6	−0.05	1.00
4.03 M	0.273 ± 0.002	0.745 ± 0.001	5	1.97	1.03

*n, number of decays analyzed simultaneously.

TABLE 2 Rate constants of PBFI estimated by global compartmental analysis

k_{01} $(ns)^{-1}$	1.102 ± 0.001
k_{21} $(M\ ns)^{-1}$	0.269 ± 0.007
k_{02} $(ns)^{-1}$	1.80 ± 0.01
k_{12} $(ns)^{-1}$	1.369 ± 0.009

By using the rate constant values of Table 2 the decay times can be calculated as a function of $[K^+]$ according to Eqs. 6–8. These decay times are plotted in Fig. 2 as a function of $-\log[K^+]$ together with the decay times estimated directly from global biexponential analysis. There is a good agreement between these two sets of decay times.

By using the values of k_{01}, k_{02}, and the quantum yields of fluorescence ϕ for the K^+ free and bound forms of PBFI, the rate constant values for fluorescence and nonradiative decay for the K^+ free and bound forms of PBFI can be calculated (Table 3). The values for ϕ are 0.024 and 0.072 for the K^+ free and bound forms of PBFI, respectively (Minta and Tsien, 1989). Although both radiative and nonradiative rate constants increase upon binding, the radiative rate constant increases relatively more than the nonradiative rate constant. This accounts for the increase in the fluorescence intensity when $[K^+]$ increases.

From k_{12}/k_{21} the dissociation constant K_d^* in the excited state was calculated, yielding a value of 5.09 M ($pK_d^* = -0.71$). In comparison with the ground-state equilibrium ($pK_d = 2.18$) the excited state is more dissociative.

To investigate the interference of the excited-state reaction with the determination of K_d and/or $[K^+]$, fluorimetric titration curves F (Eq. 11) were simulated for two excitation wavelengths (345 nm and 385 nm) and one common emission wavelength (510 nm) assuming the presence and absence of an excited-state reaction. The estimated values of k_{01}, k_{21}, k_{02}, and k_{12} (Table 2) were used together with the following experimentally determined values of K_d = 6.62 mM; ϵ_1 = 28,000 $M^{-1}\ cm^{-1}$ and ϵ_2 = 37,300 $M^{-1}\ cm^{-1}$ at λ^{ex} = 345 nm; ϵ_1 = 3,500 $M^{-1}\ cm^{-1}$ and ϵ_2 = 3,900 $M^{-1}\ cm^{-1}$ at λ^{ex} = 385 nm; $c_1/(c_1 + c_2) = 0.37$, $c_2/(c_1 + c_2) = 0.63$ at 510 nm. The resulting fluorimetric titration curves F versus $-\log[K^+]$ are shown in Fig. 3. In the absence of an excited-state reaction the only inflection point occurs at $[K^+] = K_d$ = 6.62 mM. In the presence of the excited-state reaction, in addition to the inflection point at $[K^+] = K_d$ there are two extra inflection points (at $[K^+]$ = 1.12 M and 6.31 M). Thus, the inflection point at $[K^+] = K_d$ is independent of the presence or absence of the excited-state reaction. Therefore, fluorimetric titration, can be safely used to determine K_d and/or K^+ concentration.

TABLE 3 Radiative (k_F) and nonradiative (k_{NR}) deactivation rate constant values of the K^+ free and bound forms of PBFI

Species	ϕ*	k_F $(ns)^{-1}$	k_{NR} $(ns)^{-1}$
Free form (1)	0.024	0.026 ± 0.001	1.075 ± 0.002
Bound from (2)	0.072	0.130 ± 0.001	1.67 ± 0.01

*Fluorescence quantum yield values taken from Minta and Tsien (1989).

The experimental fluorimetric titration curve F(510 nm, 345 nm) as function of $-\log[K^+]$ is represented in Fig. 4. Also shown are the simulated fluorimetric titration curves F(510 nm, 345 nm), calculated by assuming the presence or absence of an excited-state reaction. The rate constant values of Table 2 are used, together with K_d = 6.62 mM; ϵ_1 = 28,000 $M^{-1}\ cm^{-1}$ and ϵ_2 = 37,300 $M^{-1}\ cm^{-1}$ at λ^{ex} = 345 nm; $c_1/(c_1 + c_2) = 0.37$, $c_2/(c_1 + c_2) = 0.63$ at 510 nm. The inflection point of the experimental titration curve occurs at $[K^+] = K_d$.

CONCLUSIONS

We have investigated the reversible excited-state reaction between PBFI and K^+ using both steady-state and time-resolved fluorescence. By using global compartmental analysis it was possible to determine the four rate constants of the excited-state reaction. From the estimated values of k_{12} and k_{21} the dissociation constant K_d^* was calculated. It was found that pK_d^* is smaller than pK_d by approximately three units. The interference of the excited-state reaction can be neglected in the determination of K_d and/or the K^+ concentration from fluorimetric titrations.

K. M. is a predoctoral fellow of the Instituut tot Aanmoediging van het Wetenschappelijk Onderzoek in de Nijverheid en de Landbouw (IWONL). N. B. is an Onderzoeksleider of the Fonds voor Geneeskundig Wetenschappelijk Onderzoek (FGWO). The continuing support of the Ministry of Scientific Programming through IUAP-II-16 is gratefully acknowledged.

REFERENCES

Ameloot, M., N. Boens, R. Andriessen, V. Van den Bergh, and F. C. De Schryver. 1991. Non a priori analysis of fluorescence decay surfaces of excited-state processes. I. Theory. *J. Phys. Chem.* 95:2041–2047.

Ameloot, M., N. Boens, R. Andriessen, V. Van den Bergh, and F. C. De Schryver. 1992. Compartmental analysis of fluorescence decay surfaces of excited-state processes. *Methods Enzymol.* 210:314–340.

Boens, N. 1991. Pulse fluorometry. *In* Luminescence Techniques in Chemical and Biochemical Analysis. W. R. G. Baeyens, D. De Keukeleire, and K. Korkidis, editors. Dekker, New York. 21–45.

Boens N., L. D. Janssens, and F. C. De Schryver. 1989. Simultaneous analysis of single-photon timing data for the one-step determination of activation energies, frequency factors and quenching rate constants: application to tryptophan photophysics. *Biophys. Chem.* 33:77–90.

Kowalczyk A., N. Boens, V. Van den Bergh, and F. C. De Schryver. 1994. Determination of the ground-state dissociation constant by fluorimetric titration. *J. Phys. Chem.* 98:8585–8590.

Kuipers, O. P., M. Vincent, J. C. Brochon, H. M. Verheij, G. H. De Haas, and J. Gallay. 1991. Insight into the conformational dynamics of specific regions of porcine pancreatic phospholipase A_2 from a time-resolved fluorescence study of a genetically inserted single tryptophan residue. *Biochemistry.* 30:8771–8785.

Marquardt, D. W. 1963. An algorithm for least-squares estimation of nonlinear parameters. *J. Soc. Industr. Appl. Math.* 11:431–441.

Minta, A., and R. Y. Tsien. 1989. Fluorescent indicators for cytosolic sodium. *J. Biol. Chem.* 264:19449–19475.

O'Connor, D. V., and D. Phillips. 1984. *Time-Correlated Single Photon Counting.* Academic Press, London.

Smith, B. T., J. M. Boyle, B. S. Garbow, Y. Ikebe, V. C. Klema, and C. B. Moler. 1974. *In* Lecture Notes in Computer Science, Vol. 6. G. Goos and J. Hartmanis, editors. Springer-Verlag, Berlin.

Van den Bergh, V., A. Kowalczyk, N. Boens, and F. C. De Schryver. 1994. Experimental design in the global compartmental analysis of intermolecular two-state excited-state processes. *J. Phys. Chem.* 98:9503–9508.